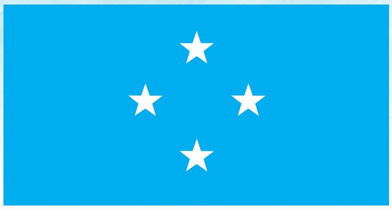

Bill Jaynes, FSM

Chapter 4
Federated States of Micronesia

4.1 Climate Summary

4.1.1 Current Climate

- Warming trends are evident in annual and half-year mean air temperatures for Pohnpei since 1951. The Yap mean air temperature trend shows little change for the same period.
- Extreme temperatures such as Warm Days and Warm Nights have been increasing at Pohnpei consistent with global warming trends. Trends in minimum temperatures at Yap are not consistent with Pohnpei or global warming trends and may be due to unresolved inhomogeneities in the record.
- At Pohnpei, there has been a decreasing trend in May–October rainfall since 1950. This implies either a shift in the mean location of the Inter-Tropical Convergence Zone (ITCZ) away from Pohnpei and/or a change in the intensity of rainfall associated with the ITCZ.
- There has also been a decreasing trend in Very Wet Day rainfall at Pohnpei and Consecutive Dry Days at Yap since 1952. The remaining annual, half-year and extreme daily rainfall trends show little change at both sites.
- Tropical cyclones (typhoons) affect the Federated States of Micronesia mainly between June and November. An average of 71 cyclones per decade developed within or crossed the Federated States of Micronesia's Exclusive Economic Zone (EEZ) between the 1977 and 2011 seasons. Tropical cyclones were most frequent in El Niño years (88 cyclones per decade) and least frequent in La Niña years (38 cyclones per decade). The neutral season average is 84 cyclones per decade. Thirty-seven of the 212 tropical cyclones (17%) between the 1981 and 2011 seasons became severe events (Category 3 or stronger) in the Federated States of Micronesia's EEZ. Available data are not suitable for assessing long-term trends.
- Wind-waves in the Federated States of Micronesia are dominated by north-easterly trade winds and westerly monsoon winds seasonally, and the El Niño–Southern Oscillation (ENSO) interannually. There is little variation in wave climate between the eastern and western parts of the country; however Yap, in the west, has a more marked dependence on the El Niño–Southern Oscillation in June–September than Pohnpei, in the east. Available data are not suitable for assessing long-term trends (see Section 1.3).

4.1.2 Climate Projections

For the period to 2100, the latest global climate model (GCM) projections and climate science findings indicate:

- El Niño and La Niña events will continue to occur in the future (*very high confidence*), but there is little consensus on whether these events will change in intensity or frequency;
- Annual mean temperatures and extremely high daily temperatures will continue to rise (*very high confidence*);
- Average annual rainfall is projected to increase (*medium confidence*), with more extreme rain events *(high confidence*);
- Drought frequency is projected to decrease (*medium confidence*);
- Ocean acidification is expected to continue *(very high confidence);*
- The risk of coral bleaching will increase in the future (*very high confidence);*
- Sea level will continue to rise *(very high confidence); and*
- Wave height is projected to decrease in December–March *(low confidence)*, and waves may be more directed from the south in the June–September *(low confidence)*.

4.2 Data Availability

There are 23 operational meteorological stations in the Federated States of Micronesia. Multiple observations within a 24-hour period are taken at five stations in Chuuk State, six in Pohnpei State (including Kosrae State) and three in Yap State. In addition, there are two single-observation-a-day climate stations in Pohnpei and seven single-observation-a-day rainfall stations in Yap. Rainfall data for Pohnpei are available from 1949 and Yap from 1951. Air temperature data are available from 1950 for Pohnpei and 1951 for Yap.

The complete historical rainfall and air temperature records for Pohnpei and Yap have been used in this report. These records are considered homogeneous given the available metadata, however low confidence is given to Yap's minimum air temperature data that remain inconsistent with temperature records in the region, likely due to remaining inhomogeneities in the record. Additional information on historical climate trends in the Federated States of Micronesia region can be found in the Pacific Climate Change Data Portal www.bom.gov.au/climate/pccsp/.

Wind-wave data from buoys are particularly sparse in the Pacific region, with very short records. Model and reanalysis data are therefore required to detail the wind-wave climate of the region. Reanalysis surface wind data have been used to drive a wave model over the period 1979–2009 to generate a hindcast of the historical wind-wave climate.

4.3 Seasonal Cycles

Information on temperature and rainfall seasonal cycles can be found in Australian Bureau of Meteorology and CSIRO (2011).

4.3.1 Wind-driven Waves

Surface wind-wave driven processes can impact on many aspects of Pacific Island coastal environments, including: coastal flooding during storm wave events; coastal erosion, both during episodic storm events and due to long-term changes in integrated wave climate; characterisation of reef morphology and marine habitat/species distribution; flushing and circulation of lagoons; and potential shipping and renewable wave energy solutions. The surface offshore wind wave climate can be described by characteristic wave heights, lengths (wave period) and directions.

In the eastern Federated States of Micronesia (e.g. on the north coast of Pohnpei), waves are predominantly directed from the north-east throughout the year, but display strong seasonal variability of direction with increased variability in direction during June–September (Figure 4.1). Wave heights and periods also vary seasonally, reaching a maximum in December–March (mean wave height 7’1” (2.2 m) and period 8.7 s), with minima around the start of the wetter season (June–September) (seasonal mean wave height 3’9” (1.1 m) and period 7.8 s) (Table 4.1). The wave climate is characterised by trade wind generated waves from the north-east and east. During December–March swell is propagated from storm events in the north-west from monsoons and North Pacific extra-tropical storms. In June–September swell waves are generated from Southern Hemisphere storms and occasionally from the south-east from trade winds. Waves larger than 10’2” (3.1 m) (99th percentile) to the north of Pohnpei occur predominantly between November and April and have longer than average periods, usually directed from the north-east to north-west, associated with typhoons and extra-tropical storms. The height of a 1-in-50 year wave event on the north coast of Pohnpei is calculated to be 19’2” (5.8 m).

In the western Federated States of Micronesia (e.g. on the south coast of Yap), waves are characterised by variability of the Northern Hemisphere trade winds and westerly monsoon winds. During the northern trade wind season, December–March, waves at Yap are east-northeasterly and have a larger height and slightly longer period than in other months (mean height around 5’1” (1.5 m) and period around 7.5 s), with some north-westerly swell from extra-tropical storms (Figure 4.2). In the wetter months of June–September, waves have a slightly shorter period (mean around 7.2 s) and lower height (mean around 3’6” (1.1 m) than December–March (Table 4.1). These waves consist of locally generated trade wind waves from the east and north-east, as well as locally generated westerly monsoon waves and easterly trade wind swell. Waves larger than 9’6” (2.9 m) (99th percentile) occur from the south-west in the wetter months due to monsoon systems and typhoons, and from the west, east, and varying directions in November–March from extra-tropical storms. The height of a 1-in-50 year wave event on the south coast of Yap is calculated to be 31’3” (9.5 m).

No suitable dataset is available to assess long-term historical trends in wave climate for the Federated States of Micronesia. However, interannual variability may be assessed in the hindcast record. The wind-wave climate displays strong interannual variability at both Pohnpei and Yap, varying with the El Niño–Southern Oscillation (ENSO) in June–September. During La Niña years, mean wave power at Pohnpei is greater than during El Niño years in June–September, and waves are more strongly directed from the east, associated with increased trade wind speeds. At Yap, wave power does not vary substantially between in El Niño and La Niña years in December–March, but in June–September much weaker waves are directed from the east in La Niña years but stronger and from the west in El Niño years, associated with movement of the Inter-Tropical Convergence Zone (ITCZ) influencing changes in the trade winds and monsoon systems.

Table 4.1: Mean wave height, period and direction from which the waves are travelling around the Federated States of Micronesia in December–March and June–September. Observation (hindcast) and climate model simulation mean values are given with the 5–95th percentile range (in brackets). Projections are made for eastern and western area averages of the Federated States of Micronesia, so historical model simulation values are given for these areas for comparison (see Section 4.5.6 – Wind driven waves, and Tables 4.8 and 4.9). A compass relating number of degrees to cardinal points (direction) is shown.

		Hindcast Reference Data (1979–2009), north Pohnpei	Climate Model Simulations (1986–2005) – Eastern Federated States of Micronesia	Hindcast Reference Data (1979–2009), south Yap	Climate Model Simulations (1986–2005) – Western Federated States of Micronesia
Wave Height (metres)	December–March	2.2 (1.5–2.9)	2.0 (1.7–2.4)	1.5 (1.0–2.2)	1.8 (1.5–2.2)
	June–September	1.1 (0.7–1.6)	1.1 (0.9–1.4)	1.1 (0.6–2.1)	1.0 (0.8–1.3)
Mean wave height (feet)	December–March	7.1 (5.0–9.5)	6.7 (5.5–7.8)	5.1 (3.1–7.4)	6.0 (4.8–7.2)
	June–September	3.7 (2.4–5.4)	3.7 (3.1–4.4)	3.5 (1.9–7.0)	3.2 (2.5–4.4)
Wave Period (seconds)	December–March	8.7 (7.3–10.7)	8.0 (7.4–8.8)	7.5 (6.3–9.3)	7.6 (7.0–8.2)
	June–September	7.8 (6.3–9.7)	7.2 (6.5–7.9)	7.2 (5.7–8.8)	6.6 (6.0–7.1)
Wave direction (degrees clockwise from North)	December–March	40 (10–60)	50 (40–60)	70 (60–90)	50 (40–60)
	June–September	40 (310–80)	110 (80–160)	130 (70–270)	100 (50–150)

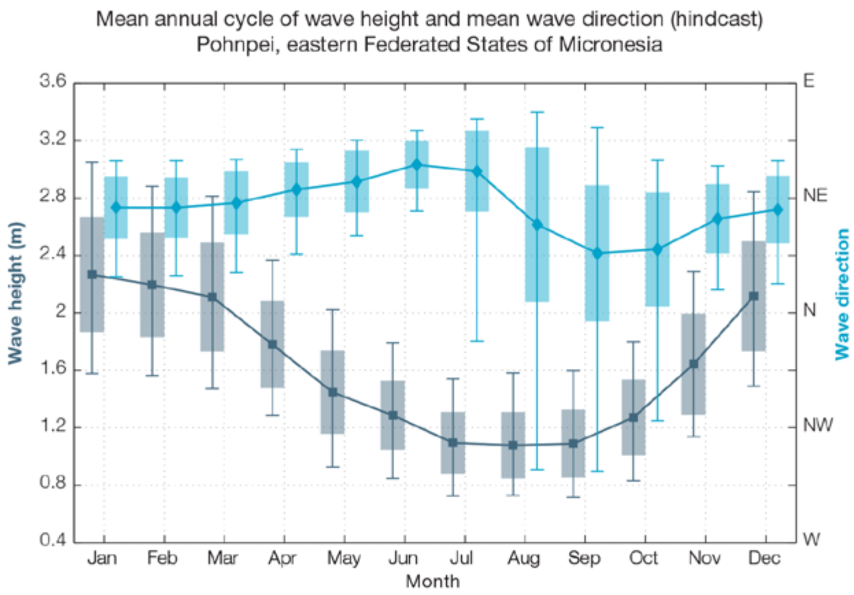

Figure 4.1: Mean annual cycle of wave height (grey) and mean wave direction (blue) at Pohnpei (eastern Federated States of Micronesia) in hindcast data (1979–2009). To give an indication of interannual variability of the monthly means of the hindcast data, shaded boxes show 1 standard deviation around the monthly means, and error bars show the 5–95% range. The direction from which the waves are travelling is shown (not the direction towards which they are travelling).

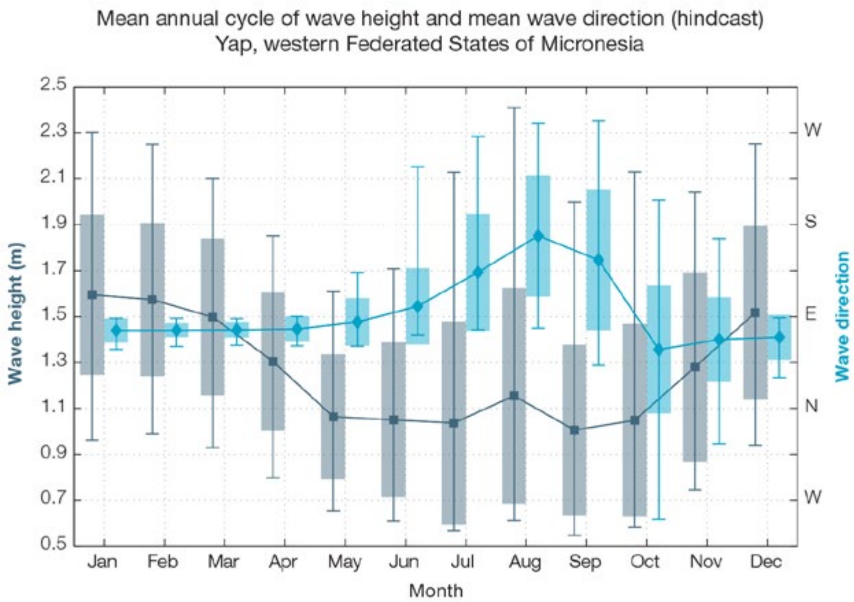

Figure 4.2: Mean annual cycle of wave height (grey) and mean wave direction (blue) at Yap (western Federated States of Micronesia) in hindcast data (1979–2009). To give an indication of interannual variability of the monthly means of the hindcast data, shaded boxes show 1 standard deviation around the monthly means, and error bars show the 5–95% range. The direction from which the waves are travelling is shown (not the direction towards which they are travelling).

4.4 Observed Trends

4.4.1 Air Temperature

Annual and Half-year Mean Air Temperature

Trends for annual and half-year mean temperatures are positive at Pohnpei with little change observed at Yap (Figure 4.3, Figure 4.4 and Table 4.2). At Pohnpei and Yap the warming trends in maximum annual and half-year air temperatures are statistically significant at the 5% level and consistent with regional and global warming trends. Minimum temperatures show significant positive trends at Pohnpei over November–April and May–October. Also at Pohnpei, annual and half-year trends in maximum air temperature are greater than those observed in minimum air temperature. The cooling trends in Yap annual and half-year minimum temperatures are inconsistent with regional and global trends. This could potentially be due to remaining inhomogeneities in record which cannot be resolved due to lack of metadata. Strong cooling trends in the minimum air temperature are responsible for no significant trends in the mean air temperatures at Yap.

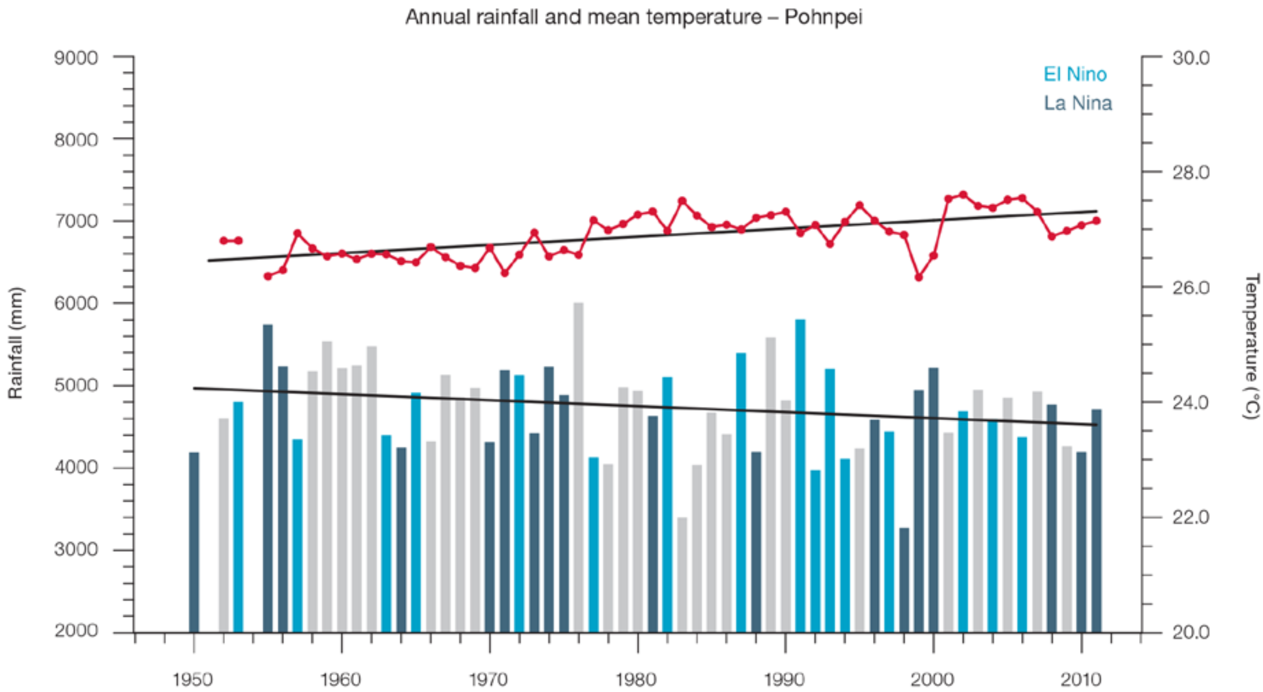

Figure 4.3: Observed time series of annual average values of mean air temperature (red dots and line) and total rainfall (bars) at Pohnpei. Light blue, dark blue and grey bars denote El Niño, La Niña and neutral years respectively. Solid black trend lines indicate a least squares fit.

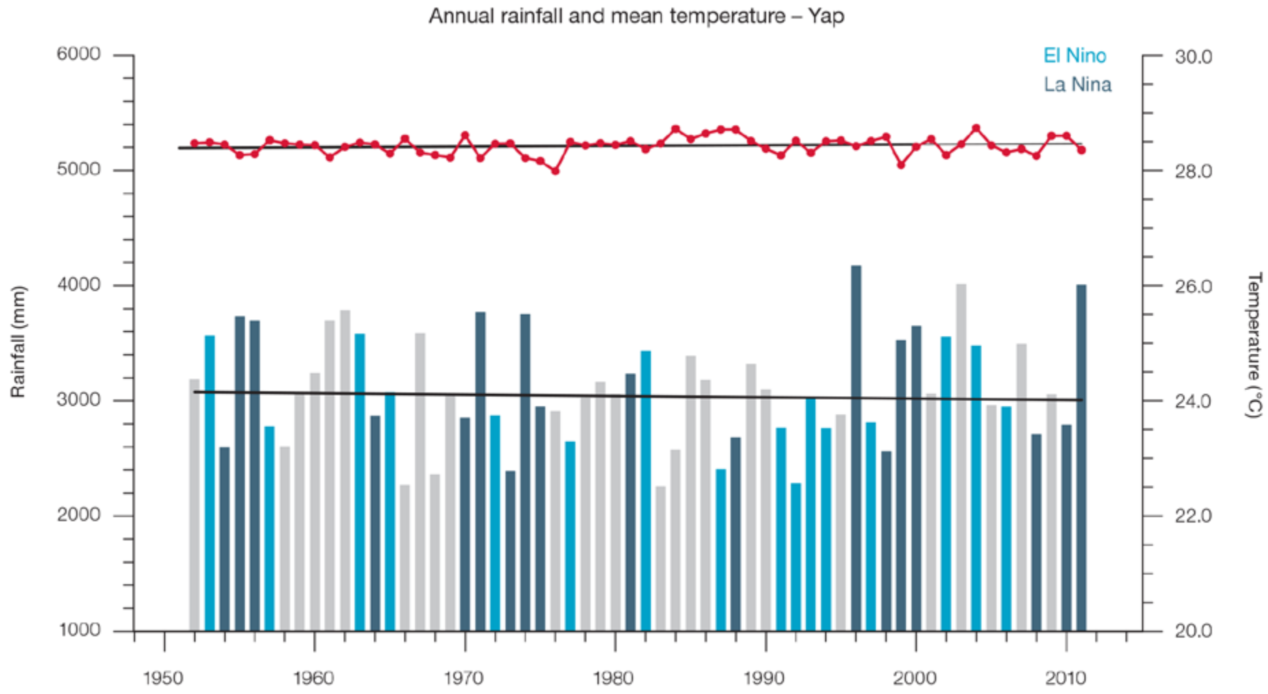

Figure 4.4: Observed time series of annual average values of mean air temperature (red dots and line) and total rainfall (bars) at Yap. Light blue, dark blue and grey bars denote El Niño, La Niña and neutral years respectively. Solid black trend lines indicate a least squares fit.

Table 4.2: Annual and half-year trends in air temperature (Tmax, Tmin, Tmean) and rainfall at Pohnpei (top) and Yap (bottom). The 95% confidence intervals are shown in parentheses. Values for trends significant at the 5% level are shown in **boldface**.

Pohnpei	**Tmax °F/10yrs [°C/10yrs]**	**Tmin °F/10yrs [°C/10yrs] 1951–2011**	**Tmean °F/10yrs [°C/10yrs]**	**Total Rain inches/10yrs [mm/10yrs] 1950–2011**
Annual	**+0.32** (+0.19, +0.46) [**+0.18** (+0.10, +0.26)]	+0.16 (-0.02, +0.35) [+0.09 (-0.01, +0.20)]	**+0.27** (+0.12, +0.38) [**+0.15** (+0.07, +0.21)]	-2.26 (-5.32, +0.61) [-57.3 (-135.1, +15.5)]
Nov–Apr	**+0.31** (+0.17, +0.48) [**+0.17** (+0.09,+0.27)]	**+0.25** (+0.03, +0.42) [**+0.14** (+0.02, +0.23)]	**+0.29** (+0.11, +0.44) [**+0.16** (+0.06, +0.25)]	-1.80 (-4.60, +1.64) [-45.8 (-116.7, +41.8)]
May–Oct	**+0.32** (+0.16, +0.46) [**+0.18** (+0.09, +0.26)]	**+0.19** (+0.03, +0.37) [**+0.11** (+0.02, +0.21)]	**+0.27** (+0.13, +0.39) [**+0.15** (+0.07, +0.22)]	**-2.23** (-4.52, -0.12) [**-56.6** (-114.9, -3.1)]

Yap	**Tmax °F/10yrs (°C/10yrs)**	**Tmin °F/10yrs (°C/10yrs) 1951–2011**	**Tmean °F/10yrs (°C/10yrs)**	**Total Rain inches/10yrs (mm/10yrs) 1952–2011**
Annual	**+0.41** (+0.36, +0.48) [**+0.23** (+0.20, +0.26)]	**-0.36** (-0.43, -0.27) [**-0.20** (-0.24, -0.15)]	+0.03 (-0.02, +0.07) [+0.01 (-0.01, +0.04)]	0.00 (-2.85, +3.22) [-0.1 (-72.5, +81.8)]
Nov–Apr	**+0.39** (+0.34, +0.44) [**+0.22** (+0.19, +0.25)]	**-0.27** (-0.37, -0.18) [**-0.15** (-0.21, -0.10)]	+0.04 (-0.02, +0.11) [+0.02 (-0.01, +0.06)]	+0.86 (-2.87, +1.44) [-21.9 (-72.8, +36.6)]
May–Oct	**+0.44** (+0.37, +0.51) [**+0.24** (+0.20, +0.28)]	**-0.40** (-0.48, -0.33) [**-0.22** (-0.27, +0.18)]	+0.01 (-0.04, +0.05) [0.00 (-0.02, +0.03)]	+0.93 (-1.27, +3.10) [+23.6 (-32.1,+78.8)]

Extreme Daily Air Temperature

Warming trends are present in the extreme indices (Table 4.3 and Figure 4.5) at Pohnpei. The annual number of Warm Days and Warm Nights has increased with Cool Days decreasing. These trends were found to be statistically significant. At Yap, Warm Days are increasing with Cool Days decreasing consistent with day-time temperature trends at Pohnpei. However, extreme minimum temperature trends show opposite trends; Cool Nights are increasing and Warm Nights decreasing – a trend that is inconsistent with mean and extreme global warming trends. This is likely due to remaining inhomogeneities in the record which could not be resolved given the metadata available at Yap.

Table 4.3: Annual trends in air temperature and rainfall extremes at Pohnpei (top) and Yap (bottom). The 95% confidence intervals are shown in parentheses. Values for trends significant at the 5% level are shown in **boldface.**

		Pohnpei	Yap
TEMPERATURE		**1952–2011**	**1952–2011**
Warm Days (days/decade)		**7.86** (+3.65, 11.70)	**12.23** (+4.60, +19.80)
Warm Nights (days/decade)		**5.12** (+1.22, +9.05)	**-16.68** (-21.57, -10.24)
Cool Days (days/decade)		**-3.98** (-5.53, -2.52)	**-8.50** (-13.66, -2.67)
Cool Nights (days/decade)		-2.73 (-8.21, +3.68)	**+8.70** (+3.71, +14.90)
RAINFALL			
Rain Days ≥ 1 mm	(days/decade)	-0.21 (-2.79, +2.48)	-1.01 (-4.20, +1.82)
Very Wet Day rainfall	(inches/decade)	**-2.63** (-5.15, -0.12)	+0.22 (-1.39, +1.97)
	(mm/decade)	**-66.88** (-130.81, -3.05)	+5.55 (-35.30, +49.95)
Consecutive Dry Days (days/decade)		0.00 (-0.43, +0.20)	**-0.37** (-0.77, 0.00)
Max 1-day rainfall	(inches/decade)	-0.015 (-0.29, 0.27)	-0.04 (-0.30, +0.21)
	(mm/decade)	-0.38 (-7.29, +6.84)	-0.88 (-7.62, +5.41)

Warm Days: Number of days with maximum temperature greater than the 90th percentile for the base period 1971–2000
Warm Nights: Number of days with minimum temperature greater than the 90th percentile for the base period 1971–2000
Cool Days: Number of days with maximum temperature less than the 10th percentile for the base period 1971–2000
Cool Nights: Number of days with minimum temperature less than the 10th percentile for the base period 1971–2000
Rain Days ≥ 1mm: Annual count of days where rainfall is greater or equal to 1mm (0.039 inches)
Very Wet Day rainfall: Amount of rain in a year where daily rainfall is greater than the 95th percentile for the reference period 1971–2000
Consecutive Dry Days: Maximum number of consecutive days in a year with rainfall less than 1mm (0.039 inches)
Max 1-day rainfall: Annual maximum 1-day rainfall

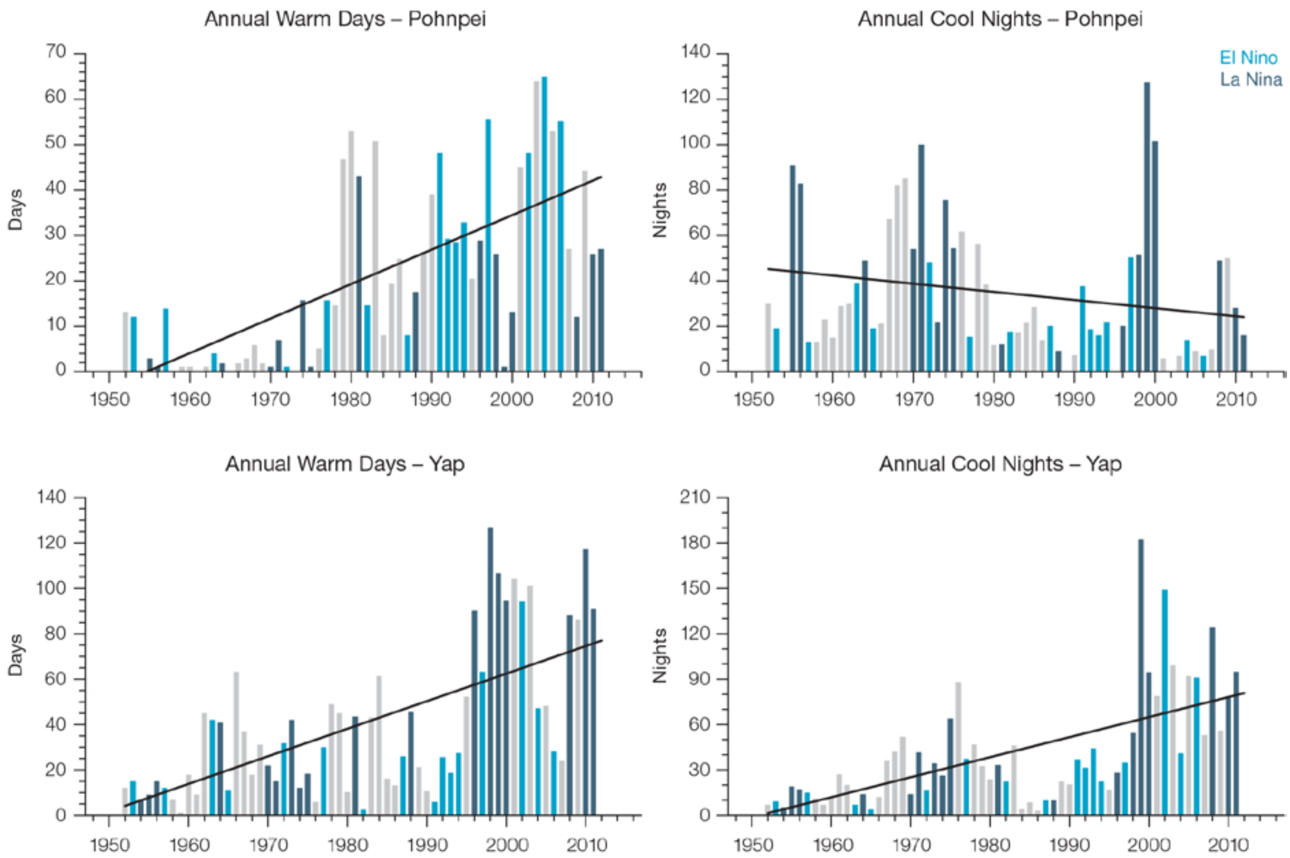

Figure 4.5: Observed time series of annual total number of Warm Days at Pohnpei (top left panel) and Yap (bottom left panel). Annual total number of Cool Nights at Pohnpei (top right panel) and Yap (bottom right panel). Solid black line indicates least squares fit.

4.4.2 Rainfall

Annual and Half-year Total Rainfall

Notable interannual variability associated with the ENSO is evident in the observed rainfall records for Pohnpei since 1950 (Figure 4.3) and Yap since 1952 (Figure 4.4). The negative trend in Pohnpei rainfall from May–October is statistically significant at the 5% level (Table 4.2). This implies either a shift in the mean location of the ITCZ away from Pohnpei and/or a change in the intensity of rainfall associated with the ITCZ. The ITCZ is closest to the equator in March–May, and furthest north during September–November, when it becomes broader, expanding both to the north and south.

The other total rainfall trends presented in Table 4.2, Figure 4.3 and Figure 4.4 are not statistically significant. In other words, excluding Pohnpei May–October rainfall, there has been little change in rainfall at Pohnpei and Yap.

Daily Rainfall

Daily rainfall trends for Pohnpei and Yap are presented in Table 4.3. Figure 4.6 shows trends in annual Very Wet Days and Consecutive Dry Days at Pohnpei and Yap. The negative trends in annual Very Wet Day rainfall at Pohnpei and annual Consecutive Dry Days at Yap are statistically significant. The decrease in annual Consecutive Dry Days at Yap does not coincide with an increase in the number of rain days. The other extreme rainfall trends in Table 4.3 are not statistically significant.

4.4.3 Tropical Cyclones

When tropical cyclones (typhoons) affect the Federated States of Micronesia they tend to do so between June and November. The tropical cyclone archive of the Northern Hemisphere indicates that between the 1977 and 2011 seasons, 248 tropical cyclones developed within or crossed the Federated States of Micronesia's EEZ. This represents an average of 71 cyclones per decade. Refer to Chapter 1, Section 1.4.2 (Tropical Cyclones) for an explanation of the difference in the number of tropical cyclones occurring in the Federated States of Micronesia in this report (Australian Bureau of Meteorology and CSIRO, 2014) compared to Australian Bureau of Meteorology and CSIRO (2011).

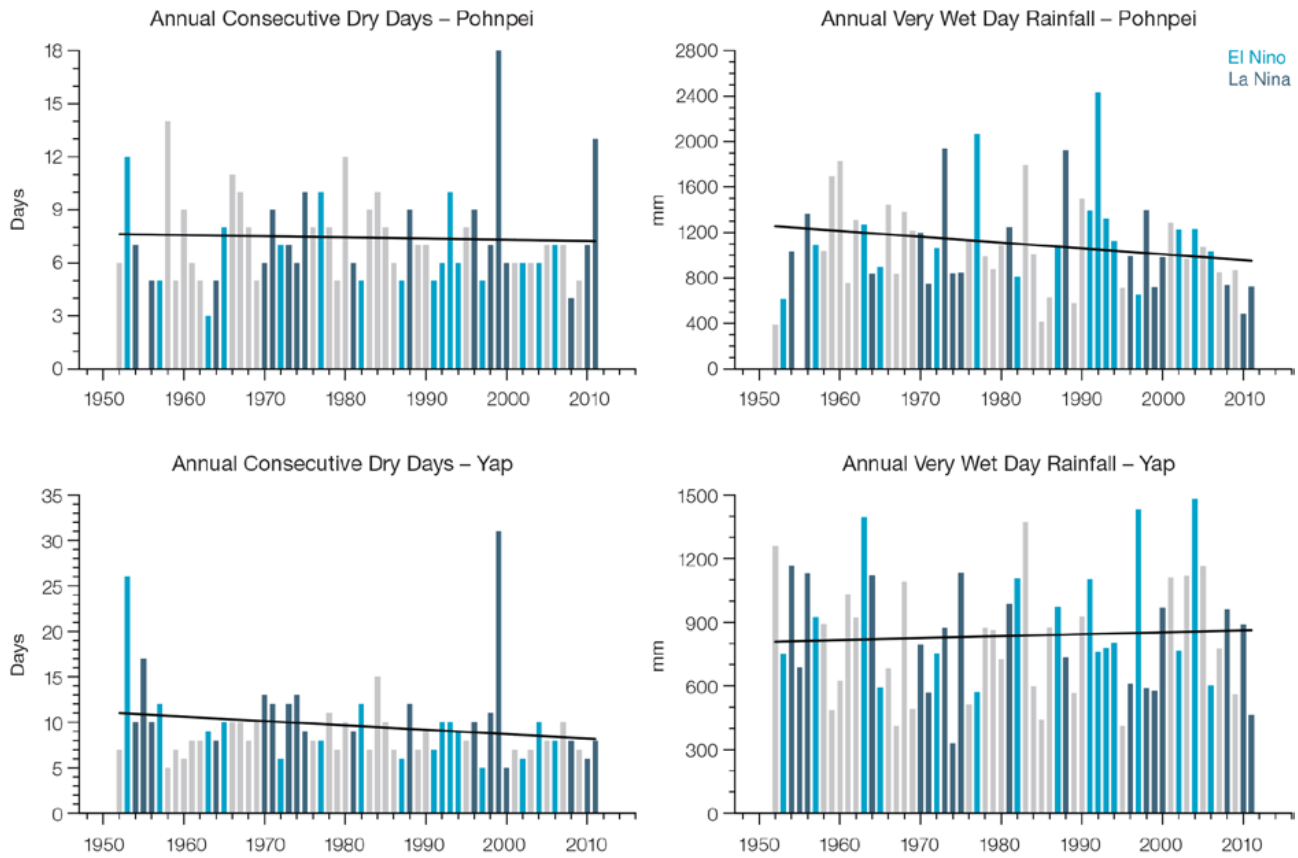

Figure 4.6: Observed time series of annual Consecutive Dry Days at Pohnpei (top left panel) and Yap (bottom left panel), and annual Very Wet Days at Pohnpei (top right panel) and Yap (bottom right panel). Solid black line indicates least squares fit.

Interannual variability in the number of tropical cyclones in the Federated States of Micronesia's EEZ is large, ranging from zero in 1999 to 12 in 1979 and 1987 (Figure 4.7). Tropical cyclones were most frequent in El Niño and neutral years, and least frequent in La Niña years. The neutral season average is 84 cyclones per decade. Thirty-seven of the 212 tropical cyclones (17%) between the 1981 and 2011 seasons became severe events (Category 3 or higher) within the Federated States of Micronesia's EEZ.

Long term trends in frequency and intensity have not been presented as country scale assessment is not recommended. Some tropical cyclone tracks analysed in this subsection include the tropical depression stage (sustained winds less than or equal to 34 knots) before and/or after tropical cyclone formation.

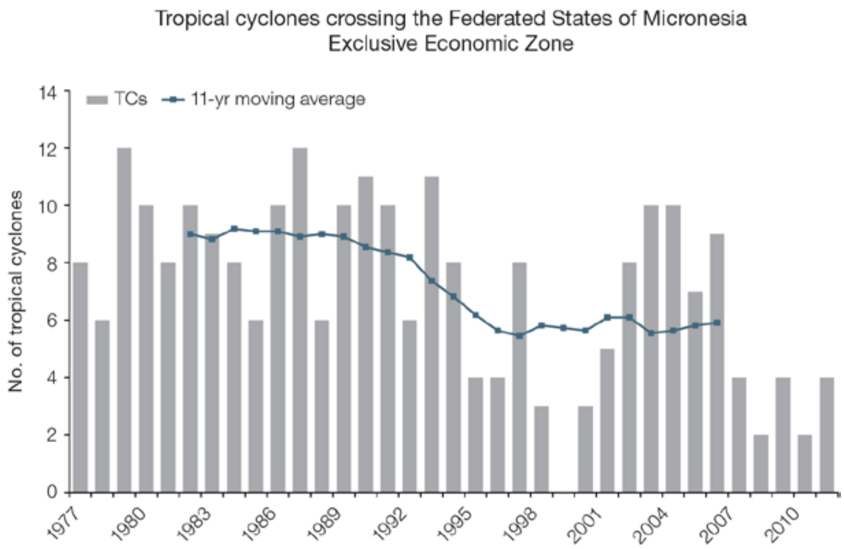

Figure 4.7: Time series of the observed number of tropical cyclones developing within and crossing the Federated States of Micronesia EEZ per season. The 11-year moving average is in blue.

4.5 Climate Projections

The performance of the available Coupled Model Intercomparison Project (Phase 5) (CMIP5) climate models over the Pacific has been rigorously assessed (Brown et al., 2013a, b; Grose et al., 2014; Widlansky et al., 2013). The simulation of the key processes and features for the Federated States of Micronesia region is similar to the previous generation of CMIP3 models, with all the same strengths and many of the same weaknesses. The best-performing CMIP5 models used here have lower biases (differences between the simulated and observed climate data) than the best CMIP3 models, and there are fewer poorly-performing models. For the Federated States of Micronesia, the most important model bias is that the simulated rainfall in the ITCZ and the West Pacific Monsoon (WPM) is too wet in November–April in the present climate, but March–October rainfall is within observed uncertainty. This affects the confidence in the model projections. Out of 27 models assessed, one model was rejected for use in these projections due to biases in the mean climate. Climate projections have been derived from up to 26 new GCMs in the CMIP5 database (the exact number is different for each scenario, Appendix A), compared with up to 18 models in the CMIP3 database reported in Australian Bureau of Meteorology and CSIRO (2011).

It is important to realise that the models used give different projections under the same scenario. This means there is not a single projected future for the Federated States of Micronesia, but rather a range of possible futures for each emission scenario. This range is described below.

4.5.1 Temperature

Further warming is expected over the Federated States of Micronesia (Figure 4.8, Tables 4.6 and 4.7). Under all RCPs, the warming is up to 1.1°C by 2030, relative to 1995, but after 2030 there is a growing difference between each RCP. For example, in the eastern Federated States of Micronesia by 2090, a warming of 2.1 to 4.1°C is projected for RCP8.5 (very high emissions) while a warming of 0.5 to 1.2°C is projected for RCP2.6 (very low emissions), with a very similar change in Western Federated States of Micronesia. The total range of projected temperatures is broader than that presented in Australian Bureau of Meteorology and CSIRO (2011) because a wider range of emissions scenarios is considered. While relatively warm and cool years and decades will still occur due to natural variability, there is projected to be more warm years and decades on average in a warmer climate.

There is *very high confidence* that temperatures will rise because:

- It is known from theory and observations that an increase in greenhouse gases will lead to a warming of the atmosphere; and
- Climate models agree that the long-term average temperature will rise.

There is *high confidence* in the model average temperature change shown in Tables 4.6 and 4.7 because:

- The new models do a good job of simulating the rate of temperature change of the recent past; and
- There are no large model biases in sea-surface temperatures in the region.

4.5.2 Rainfall

The long-term average rainfall over the Federated States of Micronesia is projected by almost all models to increase (Figure 4.9, Table 4.6 and 4.7). Models consistently project a greater increase in rainfall in May–October rainfall than in November–April rainfall. However, the year-to-year rainfall variability over the Federated States of Micronesia is still the same or larger than the projected change, even in the highest emission scenario by 2090. Mean rainfall increased markedly in the western Federated States of Micronesia between 1979 and 2006 (Figure 4.8, bottom panel), but the models do not project this will continue at this rate into the future. This indicates that the recent increase may be caused partly by natural variability and not caused by global warming. It is also possible that the models do not simulate a key process driving the recent change. However, the recent change is not particularly large (<10%) and the observed record shown is not particularly long (28 years), so it is difficult to determine the importance of this difference, and its cause. There will still be wet and dry years and decades due to natural variability, but models show that the long-term average may be wetter in the Federated States of Micronesia by the end of the century. The effect of climate change on average rainfall may not be obvious in the short or medium term due to natural variability.

These results are similar to those from Australian Bureau of Meteorology and CSIRO (2011), however the confidence rating has been reduced from *high confidence* to *medium confidence*. The new model results and new research into drivers of climate change have there is revealed greater complexity than was found previously.

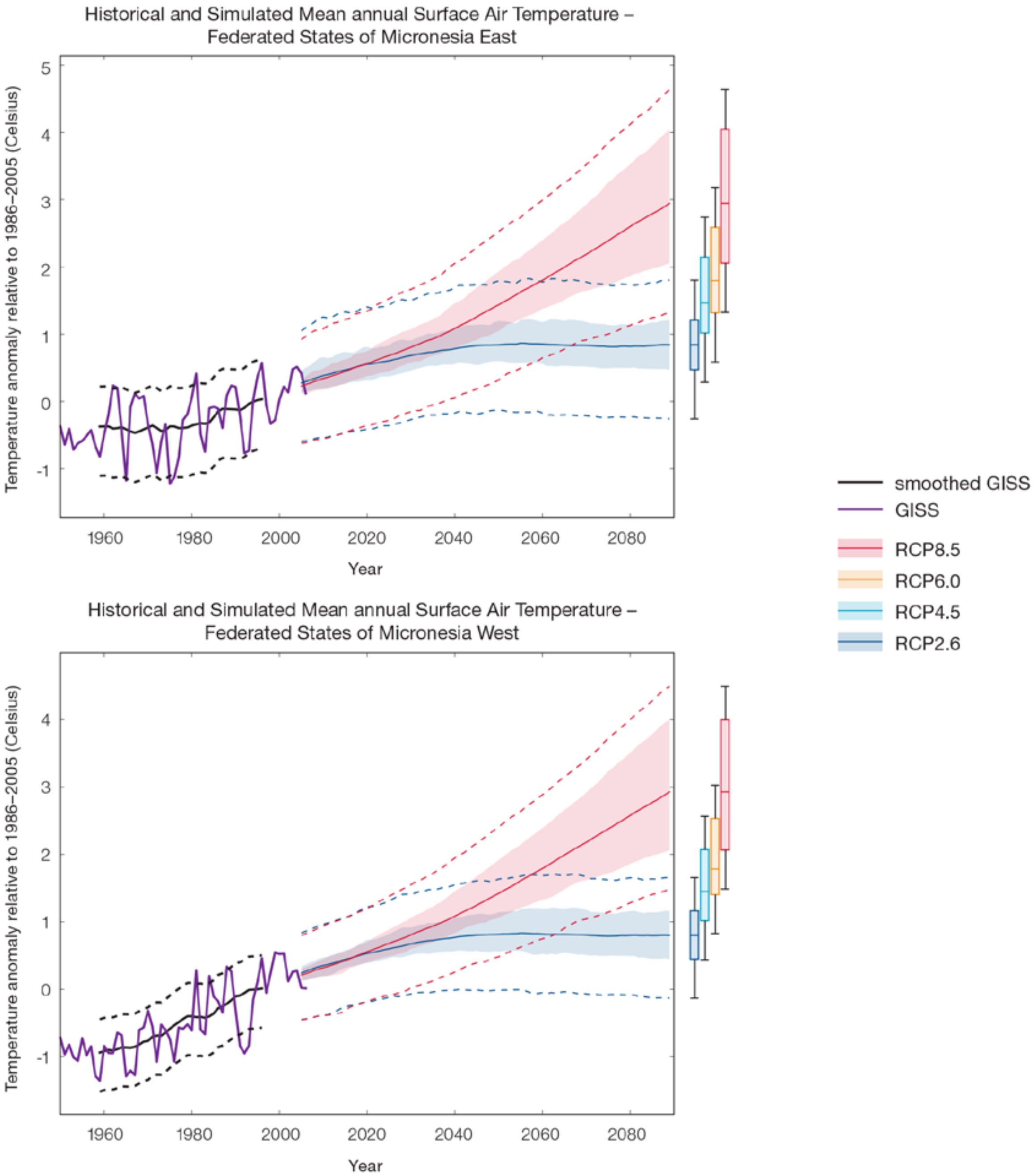

Figure 4.8: Historical and simulated surface air temperature time series for the region surrounding the eastern (top) and western (bottom) Federated States of Micronesia. The graph shows the anomaly (from the base period 1986–2005) in surface air temperature from observations (the GISS dataset, in purple), and for the CMIP5 models under the very high (RCP8.5, in red) and very low (RCP2.6, in blue) emissions scenarios. The solid red and blue lines show the smoothed (20-year running average) multi-model mean anomaly in surface air temperature, while shading represents the spread of model values (5–95th percentile). The dashed lines show the 5–95th percentile of the observed interannual variability for the observed period (in black) and added to the projections as a visual guide (in red and blue). This indicates that future surface air temperature could be above or below the projected long-term averages due to interannual variability. The ranges of projections for a 20-year period centred on 2090 are shown by the bars on the right for RCP8.5, 6.0, 4.5 and 2.6.

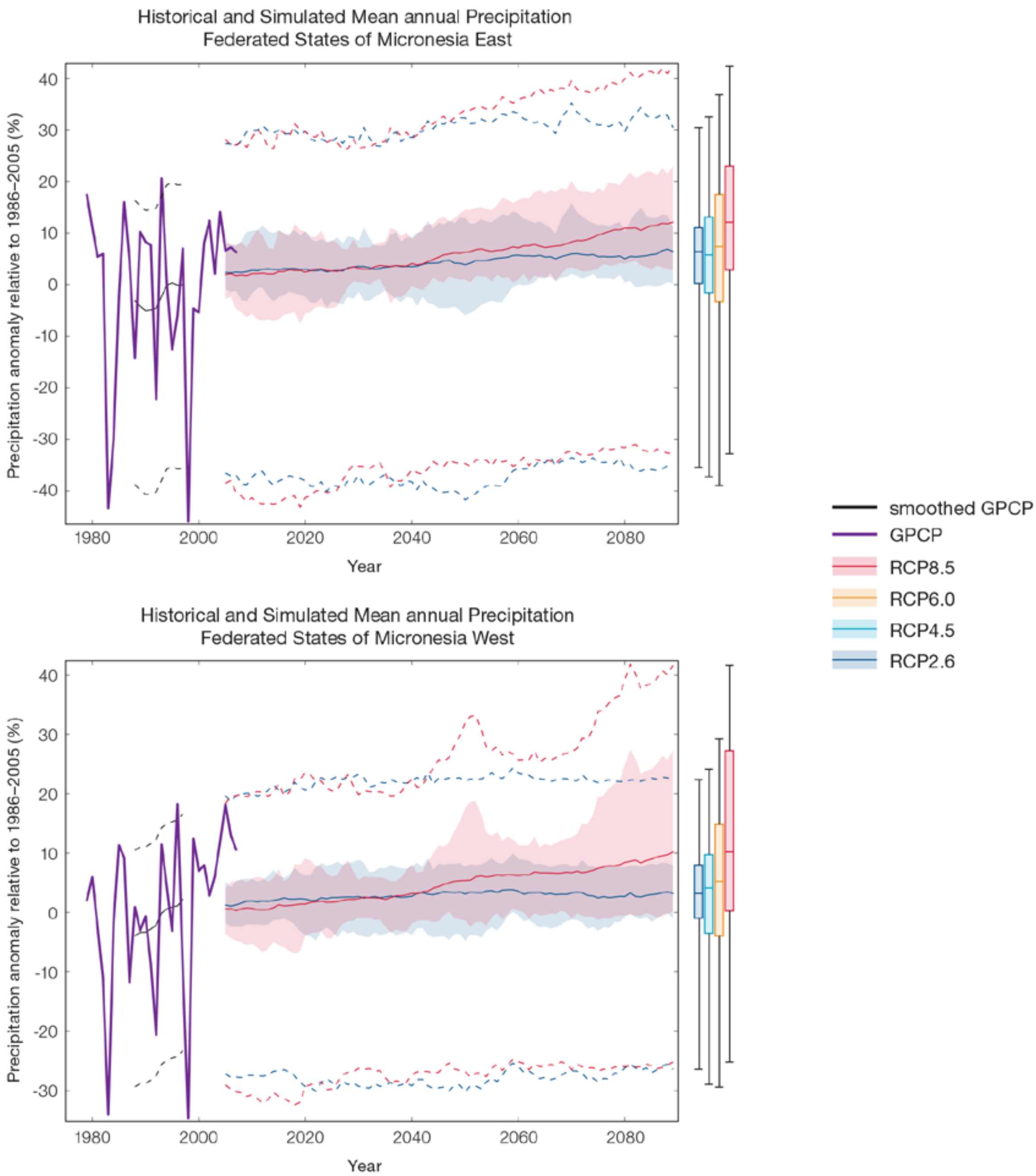

Figure 4.9: Historical and simulated annual average rainfall time series for the region surrounding the eastern (top) and western (bottom) Federated States of Micronesia. The graph shows the anomaly (from the base period 1986–2005) in rainfall from observations (the GPCP dataset, in purple), and for the CMIP5 models under the very high (RCP8.5, in red) and very low (RCP2.6, in blue) emissions scenarios. The solid red and blue lines show the smoothed (20-year running average) multi-model mean anomaly in rainfall, while shading represents the spread of model values (5–95th percentile). The dashed lines show the 5–95th percentile of the observed interannual variability for the observed period (in black) and added to the projections as a visual guide (in red and blue). This indicates that future rainfall could be above or below the projected long-term averages due to interannual variability. The ranges of projections for a 20-year period centred on 2090 are shown by the bars on the right for RCP8.5, 6.0, 4.5 and 2.6.

There is general agreement between models that rainfall will increase, and this increase is larger later in the century and for the higher emissions scenarios. There are some biases in the models in the region that lower the confidence in the amount of projected change. The 5–95th percentile range of projected values from CMIP5 climate models is moderate, e.g. for the eastern Federated States of Micronesia RCP8.5 (very high emissions) the range is 1 to +9% by 2030 and 3 to +23% by 2090.

There is *medium confidence* that the long-term rainfall over the Federated States of Micronesia will increase because:

- The majority of CMIP3 and CMIP5 models agree that the rainfall in the ITCZ and WPM will increase under a warmer climate (only two of the 27 models used showed a rainfall decrease); and
- There are well understood physical reasons why a warmer climate will lead to increased rainfall in the ITCZ region.

There is *medium confidence* in the model average rainfall change shown in Tables 4.6 and 4.7 because:

- The complex set of processes involved in tropical rainfall is challenging to simulate in models. This means that the confidence in the projection of rainfall is generally lower than for other variables such as temperature;
- Many models have a bias in November–April rainfall in the current climate; and
- The future behaviour of the El Niño–Southern Oscillation is unclear, and the El Niño–Southern Oscillation strongly influences year-to-year rainfall variability.

4.5.3 Extremes

Extreme Temperature

The temperature on extremely hot days is projected to increase by about the same amount as average temperature. This conclusion is based on analysis of daily temperature data from a subset of CMIP5 models (Chapter 1). The frequency of extremely hot days is also expected to increase.

For the eastern Federated States of Micronesia the temperature of the 1-in-20-year hot day is projected to increase by approximately 1.1°F (0.6°C) by 2030 under the RCP2.6 (very low) scenario and by 1.4°F (0.8°C) under the RCP8.5 (very high) scenario. By 2090 the projected increase is 1.4°F (0.8°C) for RCP2.6 (very low) and 5.4°F (3°C) for RCP8.5 (very high).

For the western Federated States of Micronesia the temperature of the 1-in-20-year hot day is projected to increase by approximately 1.1°F (0.6°C) by 2030 under the RCP2.6 (very low) scenario and by 1.4°F (0.8°C) under the RCP8.5 (very high) scenario. By 2090 the projected increase is 1.4°F (0.8°C) for RCP2.6 (very low) and 5.8°F (3.2°C) for RCP8.5 (very high).

There is *very high confidence* that the temperature of extremely hot days and extremely cool days will increase, because:

- A change in the range of temperatures, including the extremes, is physically consistent with rising greenhouse gas concentrations;
- This is consistent with observed changes in extreme temperatures around the world over recent decades; and
- All the CMIP5 models agree on an increase in the frequency and intensity of extremely hot days and a decrease in the frequency and intensity of cool days.

There is *low confidence* in the magnitude of projected change in extreme temperature because models generally underestimate the current intensity and frequency of extreme events. Changes to the particular driver of extreme temperatures affect whether the change to extremes is more or less than the change in the average temperature, and the changes to the drivers of extreme temperatures in the Federated States of Micronesia are currently unclear.

Extreme Rainfall

The frequency and intensity of extreme rainfall events are projected to increase. This conclusion is based on analysis of daily rainfall data from a subset of CMIP5 models using a similar method to that in Australian Bureau of Meteorology and CSIRO (2011) with some improvements (Chapter 1), so the results are slightly different to those in Australian Bureau of Meteorology and CSIRO (2011).

For the eastern Federated States of Micronesia the current 1-in-20-year daily rainfall amount is projected to increase by approximately 0.4 in (11 mm) by 2030 for RCP2.6 and by 0.6 in (15 mm) by 2030 for RCP8.5 (very high emissions). By 2090, it is projected to increase by approximately 0.8 in (20 mm) for RCP2.6 and by 1.5 in (38 mm) for RCP8.5 (very high emissions).The majority of models project the current 1-in-20-year daily rainfall event will become, on average, a 1-in-7-year event for RCP2.6 and a 1-in-6-year event for RCP8.5 (very high emissions) by 2090.

For the western Federated States of Micronesia the current 1-in-20-year daily rainfall amount is projected to increase by approximately 0.6 in (14 mm) by 2030 for RCP2.6 and by 0.7 in (18 mm) by 2030 for RCP8.5 (very high emissions). By 2090, it is projected to increase by approximately 0.75 in (19 mm) for RCP2.6 and by 1.9 in (47 mm) for RCP8.5 (very high emissions).The majority of models project the current 1-in-20-year daily rainfall event will become, on average, a 1-in-8-year event for RCP2.6 and a 1-in-4-year event for RCP8.5 (very high emissions) by 2090. These results are different to those found in Australian Bureau of Meteorology and CSIRO (2011) because of different methods used (Chapter 1).

There is *high confidence* that the frequency and intensity of extreme rainfall events will increase because:

- A warmer atmosphere can hold more moisture, so there is greater potential for extreme rainfall (IPCC, 2012); and
- Increases in extreme rainfall in the Pacific are projected in all available climate models.

There is *low confidence* in the magnitude of projected change in extreme rainfall because:

- Models generally underestimate the current intensity of local extreme events, especially in this area due to the 'cold-tongue bias' (Chapter 1);
- Changes in extreme rainfall projected by models may be underestimated because models seem to underestimate the observed increase in heavy rainfall with warming (Min et al., 2011);
- GCMs have a coarse spatial resolution, so they do not adequately capture some of the processes involved in extreme rainfall events; and
- The Conformal Cubic Atmospheric Model (CCAM) downscaling model has finer spatial resolution and the CCAM results presented in Australian Bureau of Meteorology and CSIRO (2011) indicates a smaller increase in the number of extreme rainfall days, and there is no clear reason to accept one set of models over another.

Drought

Drought projections (defined in Chapter 1) are described in terms of changes in proportion of time in drought, frequency and duration by 2090 for very low and very high emissions (RCP2.6 and 8.5).

For both the eastern and western Federated States of Micronesia the overall proportion of time spent in drought is expected to decrease under all scenarios. Under RCP8.5 the frequency of drought in all categories is projected to decrease slightly while the duration of events is projected to stay approximately the same (Figure 4.10). Under RCP2.6 (very low emissions) the frequency of severe drought is projected to decrease slightly while the frequency of drought in all other categories is projected to remain the same. The duration of events in all drought categories is projected to stay approximately the same under RCP2.6 (very low emissions).

There is *medium confidence* in this direction of change because:

- There is *high confidence* in the direction of mean rainfall change;
- These drought projections are based upon a subset of models; and
- Like the CMIP3 models, the majority of the CMIP5 models agree on this direction of change.

There is *medium confidence* in the projections of drought frequency and duration because there is *medium confidence* in the magnitude of rainfall projections, and no consensus about projected changes in the ENSO, which directly influence the projection of drought.

Tropical Cyclones

Global Picture

There is a growing level of agreement among models that on a global basis the frequency of tropical cyclones is likely to decrease by the end of the 21st century. The magnitude of the decrease varies from 6%–35% depending on the modelling study. There is also a general agreement between models that there will be an increase in the mean maximum wind speed of cyclones by between 2% and 11% globally, and an increase in rainfall rates of the order of 20% within 100 km of the cyclone centre (Knutson et al., 2010). Thus, the scientific community has a *medium* level of confidence in these global projections.

Federated States of Micronesia

The projection is for a decrease in tropical cyclone genesis (formation) frequency for the northern basin (Figure 4.11 and Table 4.4). However the confidence level for this projection is low.

The GCMs show inconsistent results across models for changes in tropical cyclone frequency for the northern basin, using either the direct detection methodologies (CVP or CDD) or the empirical methods described in Chapter 1. The direct detection methodologies tend to indicate a decrease in formation with almost half of results suggesting decreases of between 20 and 50%. The empirical techniques assess changes in the main atmospheric ingredients known to be necessary for tropical cyclone formation. About four-fifths of results suggest the conditions for tropical cyclone formation will become more favourable in this region. However, when only the models for which direct detection and empirical methods are available are considered, the assessment is for a decrease in tropical cyclone formation. These projections are consistent with those of Australian Bureau of Meteorology and CSIRO (2011).

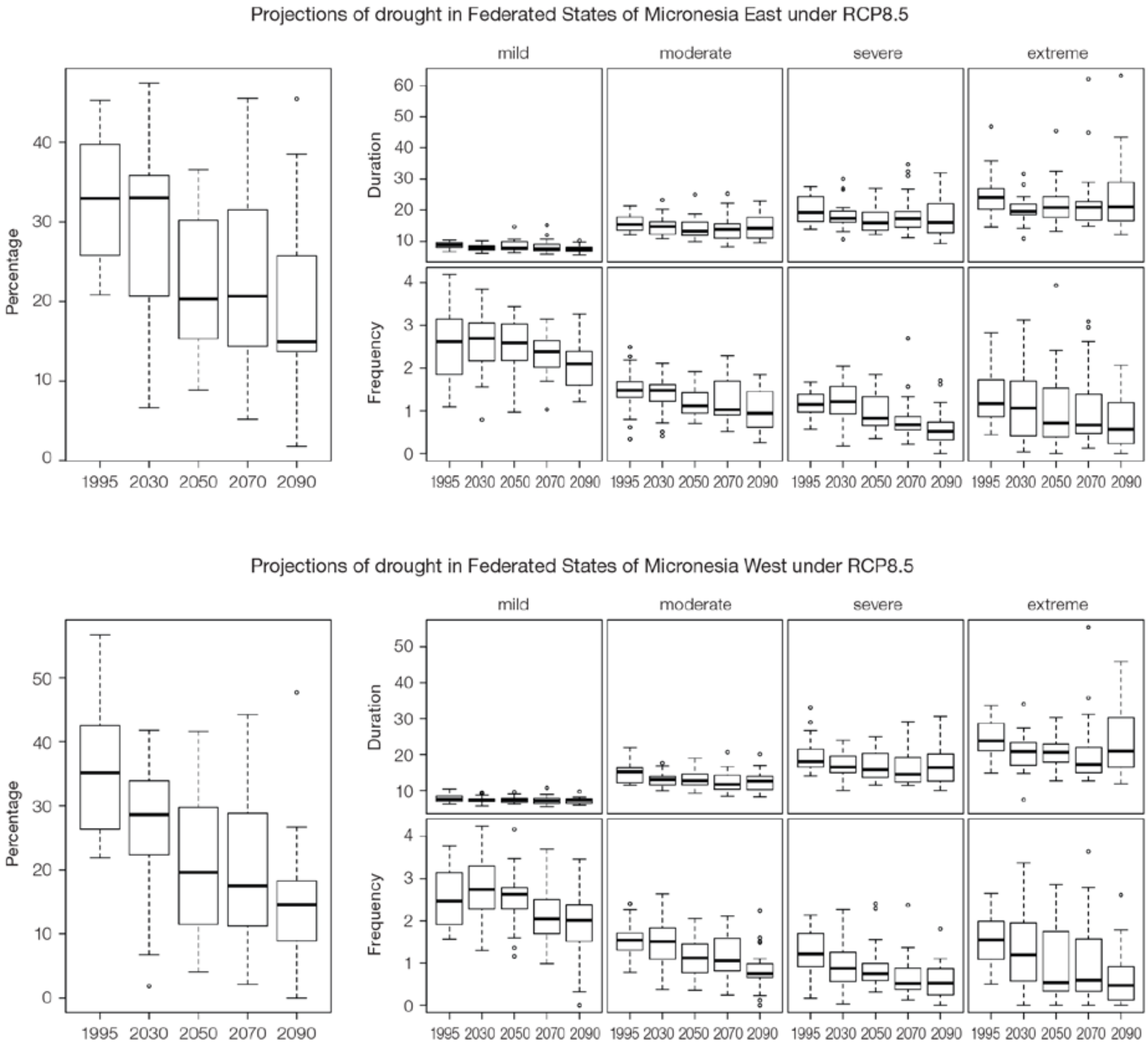

Figure 4.10: Box-plots showing percent of time in moderate, severe or extreme drought (left hand side), and average drought duration and frequency for the different categories of drought (mild, moderate, severe and extreme) for the eastern (top) and western (bottom) Federated States of Micronesia. These are shown for 20-year periods centred on 1995, 2030, 2050, 2070 and 2090 for the RCP8.5 (very high emissions) scenario. The thick dark lines show the median of all models, the box shows the interquartile (25–75%) range, the dashed lines show 1.5 times the interquartile range and circles show outlier results.

Table 4.4: Projected percentage change in cyclone frequency in the northern basin (0–15°N; 130–180°E) for 22 CMIP5 climate models, based on five methods, for 2080–2099 relative to 1980–1999 for RCP8.5 (very high emissions). The 22 CMIP5 climate models were selected based upon the availability of data or on their ability to reproduce a current-climate tropical cyclone climatology (See Section 1.5.3 – Detailed Projection Methods, Tropical Cyclones). Blue numbers indicate projected decreases in tropical cyclone frequency, red numbers an increase. MMM is the multi-model mean change. N increase is the proportion of models (for the individual projection method) projecting an increase in cyclone formation.

Model	GPI change	GPI-M change	Tippett	CDD	OWZ
access10	71	22	-54	71	
access13	55	48	-33	107	
bcccsm11	13	11	-22		2
canesm2	34	22	-47	24	
ccsm4				-81	-12
cnrm_cm5	0	-2	-25	-1	-23
csiro_mk36	7	-1	-30	8	15
fgoals_g2	-5	-15	-10		
fgoals_s2	-3	-3	-35		
gfdl-esm2m				-2	-8
gfdl_cm3	15	5	-17		-40
gfdl-esm2g				-33	-37
gisse2r	14	9	-17		
hadgem2_es	13	1	-57		
inm	25	26	-5		
ipslcm5alr	19	9	-17		
ipslcm5blr				-49	
miroc5				-52	-50
mirocesm	17	2	26		
mpim	19	17	-45		
mricgcm3	1	-3	-34		
noresm1m	-11	-17	-19	-42	
MMM	17	8	-26	-5	-19
N increase	0.8	0.7	0.1	0.4	0.3

4.5.4 Coral Reefs and Ocean Acidification

As atmospheric CO_2 concentrations continue to rise, oceans will warm and continue to acidify. These changes will impact the health and viability of marine ecosystems, including coral reefs that provide many key ecosystem services (*high confidence*). These impacts are also likely to be compounded by other stressors such as storm damage, fishing pressure and other human impacts.

The projections for future ocean acidification and coral bleaching use three RCPs (2.6, 4.5, and 8.5).

Ocean acidification

In the Federated States of Micronesia, the aragonite saturation state has declined from about 4.5 in the late 18th century to an observed value of about 3.9±0.1 by 2000 (Kuchinke et al., 2014). All models show that the aragonite saturation state, a proxy for coral reef growth rate, will continue to decrease as atmospheric CO_2 concentrations increase (*very high confidence*). Projections from CMIP5 models indicate that under RCPs 8.5 (very high emissions) and 4.5 (low emissions) the median aragonite saturation state will transition to marginal conditions (3.5) around 2030.

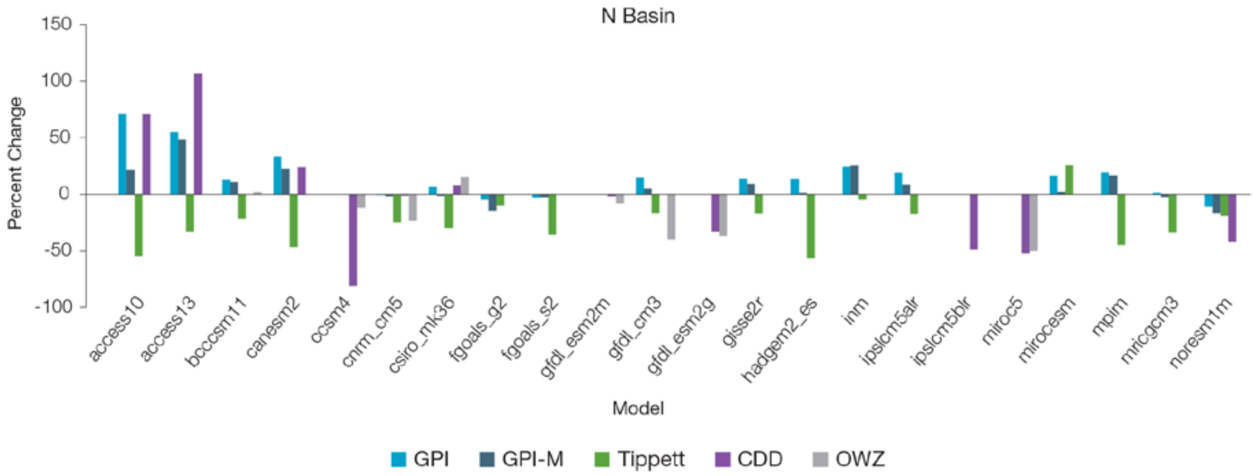

Figure 4.11: Projected percentage change in cyclone frequency in the northern basin (data from Table 4.4).

In RCP8.5 (very high emissions) the aragonite saturation state continues to strongly decline thereafter to values where coral reefs have not historically been found (< 3.0). Under RCP4.5 (low emissions) the aragonite saturation plateaus around 3.2 i.e. marginal conditions for healthy coral reefs. While under RCP2.6 (very low emissions) the median aragonite saturation state never falls below 3.5, and increases slightly toward the end of the century (Figure 4.12) suggesting that the conditions remains adequate for healthy corals reefs. There is *medium confidence* in this range and distribution of possible futures because the projections are based on climate models that do not resolve the reef scale that can play a role in modulating large-scale changes. The impacts of ocean acidification are also likely to affect the entire marine ecosystem impacting the key ecosystem services provided by reefs.

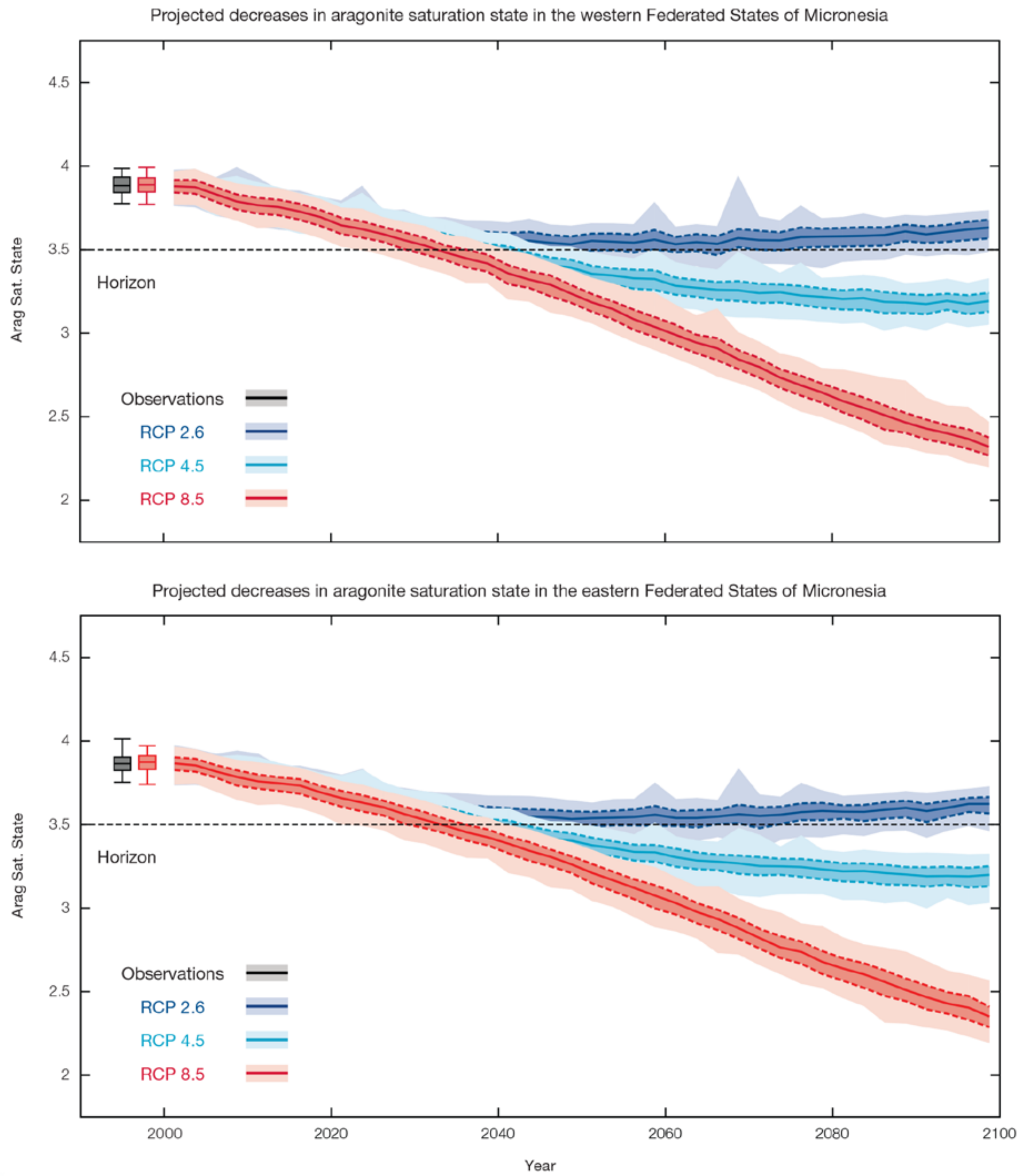

Figure 4.12: Projected decreases in aragonite saturation state in western (upper) and eastern (lower) Federated States of Micronesia from CMIP5 under RCPs 2.6, 4.5 and 8.5. Shown on this plots are the median values, the interquartile range (the dashed line), and 5% and 95% percentiles. The horizontal line represents the transition to marginal conditions for coral reef health (from Guinotte et al., 2003).

Coral Bleaching Risk

As the ocean warms, the risk of coral bleaching increases (*very high confidence).* There is *medium confidence* in the projected rate of change for the Federated States of Micronesia because there is *medium confidence* in the rate of change of SST, and the changes at the reef scale (which can play a role in modulating large-scale changes) are not adequately resolved. Importantly, the coral bleaching risk calculation does not account the impact of other potential stressors (Chapter 1).

The changes in the frequency (or recurrence) and duration of severe bleaching risk are quantified for different projected SST changes (Table 4.5). Overall there is a decrease in the time between two periods of elevated risk and an increase in the duration of the elevated risk. For example, under a long-term mean increase of 1°C (relative to 1982–1999 period), the average period of severe bleaching risk (referred to as a risk event) will last 9.4 weeks (with a minimum duration of 1.7 weeks and a maximum duration of 6.3 months) and the average time between two risks will be 1.9 years (with the minimum recurrence of 3.2 months and a maximum recurrence of 6.0 years). If severe bleaching events occur more often than once every five years, the long-term viability of coral reef ecosystems becomes threatened.

4.5.5 Sea Level

Mean sea level is projected to continue to rise over the course of the 21st century. There is *very high confidence* in the direction of change. The CMIP5 models simulate a rise of between approximately 7–18 cm by 2030 (very similar values for different RCPs), with increases of 41–90 cm by 2090 under the RCP8.5 (Figure 4.13 and Table 4.6). There is *medium confidence* in the range mainly because there is still uncertainty associated with projections of the Antarctic ice sheet contribution. Interannual variability of sea level will lead to periods of lower and higher regional sea levels. In the past, this interannual variability has been about 26 cm (5–95% range, after removal of the seasonal signal, see dashed lines in Figure 4.13 (a) and it is likely that a similar range will continue through the 21st century.

Table 4.5: Projected changes in severe coral bleaching risk for the Federated States of Micronesia EEZ for increases in SST relative to 1982–1999.

Temperature change [1]	Recurrence interval [2]	Duration of the risk event [3]
Change in observed mean	30 years	5.7 weeks
+0.25°C	26.9 years (25.4 years – 29.1 years)	5.2 weeks (4.9 weeks – 5.7 weeks)
+0.5°C	20.6 years (18.3 years – 23.3 years)	6.2 weeks (4.8 weeks – 8.8 weeks)
+0.75°C	7.4 years (2.9 years – 14.0 years)	7.2 weeks (2.7 weeks – 3.6 months)
+1°C	1.9 years (3.2 months – 6.0 years)	9.4 weeks (1.7 weeks – 6.3 months)
+1.5°C	5.4 months (1.1 months – 1.4 years)	4.6 months (1.8 weeks – 1.5 years)
+2°C	3.2 months (1.1 months – 5.4 months)	1.1 years (3.0 months – 5.1 years)

[1] This refers to projected SST anomalies above the mean for 1982–1999.
[2] Recurrence is the mean time between severe coral bleaching risk events. Range (min – max) shown in brackets.
[3] Duration refers to the period of time where coral are exposed to the risk of severe bleaching. Range (min – max) shown in brackets.

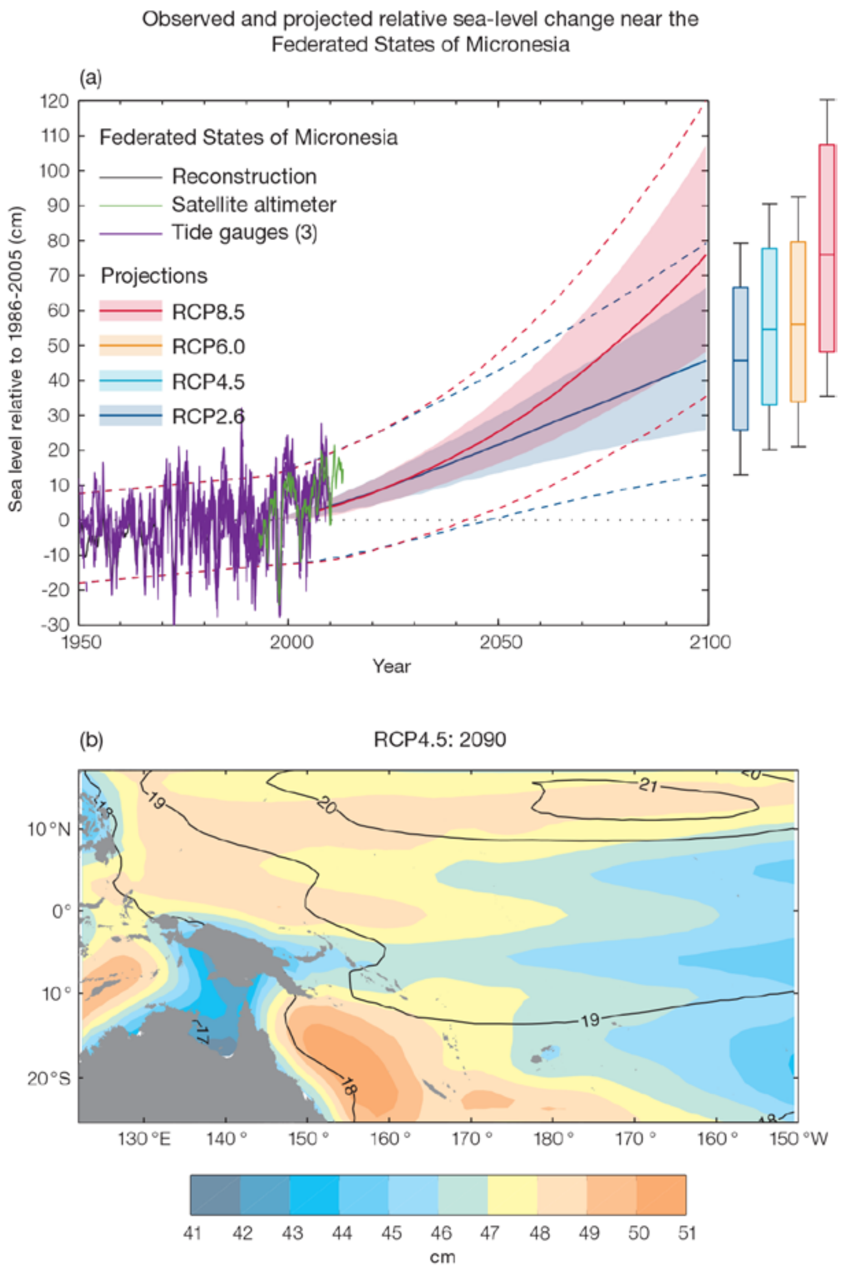

Figure 4.13: **(a)** The observed tide-gauge records of relative sea-level (since the late 1970s) are indicated in purple, and the satellite record (since 1993) in green. The gridded (reconstructed) sea level data at the Federated States of Micronesia (since 1950) is shown in black. Multi-model mean projections from 1995–2100 are given for the RCP8.5 (red solid line) and RCP2.6 emissions scenarios (blue solid line), with the 5–95% uncertainty range shown by the red and blue shaded regions. The ranges of projections for four emission scenarios (RCPs 2.6, 4.5, 6.0 and 8.5) by 2100 are also shown by the bars on the right. The dashed lines are an estimate of interannual variability in sea level (5–95% uncertainty range about the projections) and indicate that individual monthly averages of sea level can be above or below longer-term averages.

(b) The regional distribution of projected sea level rise under the RCP4.5 emissions scenario for 2081–2100 relative to 1986–2005. Mean projected changes are indicated by the shading, and the estimated uncertainty in the projections is indicated by the contours (in cm).

4.5.6 Wind-driven Waves

The projected changes in wave climate are spatially consistent across the Federated States of Micronesia.

In the western region, there is a projected decrease in December–March wave height and period (significant under RCP8.5, very high emissions in 2090) (Figure 4.14) with no change in direction *(low confidence)* (Table 4.8). In June–September there is no projected change in wave height, a small decrease in period is suggested, with a clockwise rotation toward the south implied, particularly under RCP8.5 (very high emissions) in 2090 *(low confidence)*. A decrease in the height of storm waves is suggested in December–March (*low confidence)*.

In the eastern region, projected changes in wave properties include a small decrease in wave height (significant under RCP8.5 very high emissions, by 2090) (Figure 4.15), with no change in wave period or direction during December–March (*low confidence)* (Table 4.9). During June–September, otherwise no significant changes are projected to occur in wave climate *(low confidence)*, with a suggestion of less variable wave directions. An increase in the height of storm waves is suggested in June–September *(low confidence)*.

There is *low confidence* in projected changes in the Federated States of Micronesia wind-wave climate because:

- Projected changes in wave climate are dependent on confidence in projected changes in the ENSO, which is low. and
- The differences between simulated and observed (hindcast) wave data can be larger than the projected wave changes, which further reduces our confidence in projections.

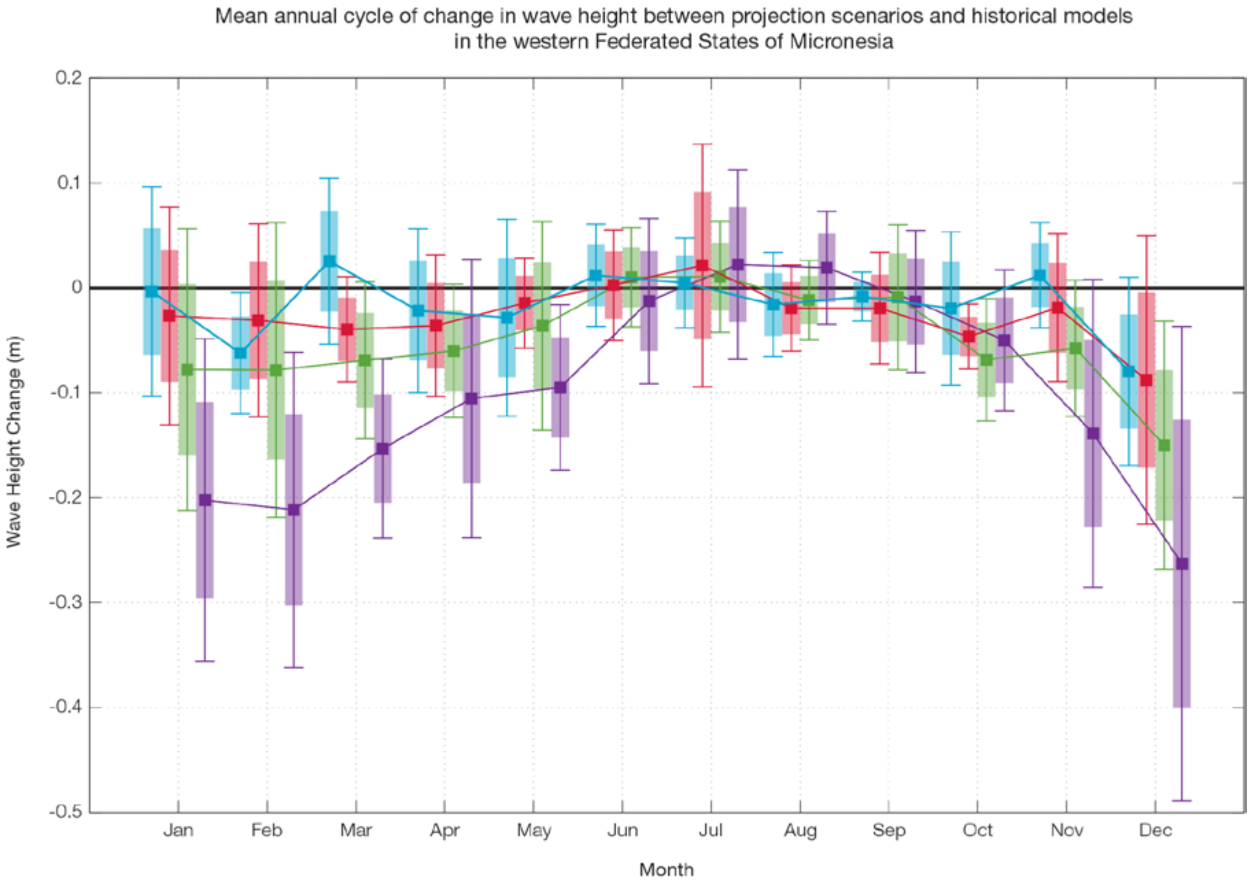

Figure 4.14: Mean annual cycle of change in wave height between projection scenarios and historical models in the western Federated States of Micronesia. This plot shows a decrease in wave heights in the dry season months (significant under RCP8.5, very high emissions by 2090), and no change in the wet season months. Shaded boxes show 1 standard deviation of models' means around the ensemble means, and error bars show the 5–95% range inferred from the standard deviation. Colours represent RCP scenarios and time periods: blue 2035 RCP4.5 (low emissions), red 2035 RCP8.5 (very high emissions), green 2090 RCP4.5 (low emissions), purple 2090 RCP8.5 (very high emissions).

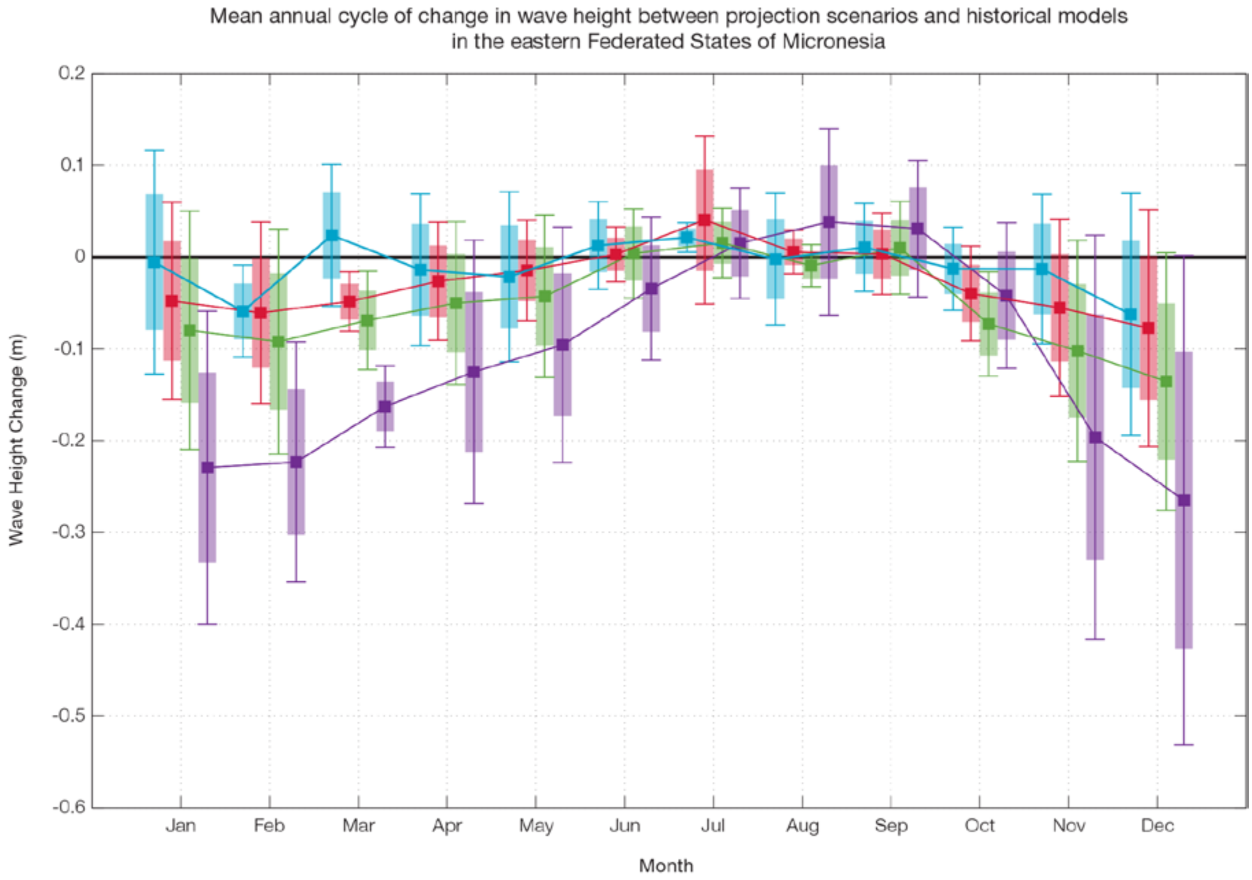

Figure 4.15: Mean annual cycle of change in wave height between projection scenarios and historical models in the eastern Federated States of Micronesia. This plot shows a decrease in wave heights in December–March (significant under RCP8.5, very high emissions, in 2090, as well as RCP4.5 2090 and RCP8.5, very high emissions, 2035 in March), and no significant change in June–September. Shaded boxes show 1 standard deviation of models' means around the ensemble means, and error bars show the 5–95% range inferred from the standard deviation. Colours represent RCP scenarios and time periods: blue 2035 RCP4.5 (low emissions), red 2035 RCP8.5 (very high emissions), green 2090 RCP4.5 (low emissions), purple 2090 RCP8.5 (very high emissions).

4.5.7 Projections Summary

There is *very high confidence* in the direction of long-term change in a number of key climate variables, namely an increase in mean and extremely high temperatures, sea level and ocean acidification. There is *high confidence* that mean annual rainfall and the frequency and intensity of extreme rainfall will increase. There is *medium confidence* that mean rainfall will increase and drought frequency will decrease.

Tables 4.6–4.9 quantify the mean changes and ranges of uncertainty for a number of variables, years and emissions scenarios. A number of factors are considered in assessing confidence, i.e. the type, amount, quality and consistency of evidence (e.g. mechanistic understanding, theory, data, models, expert judgment) and the degree of agreement, following the IPCC guidelines (Mastrandrea et al., 2010). Confidence ratings in the projected magnitude of mean change are generally lower than those for the direction of change (see paragraph above) because magnitude of change is more difficult to assess. For example, there is *very high confidence* that temperature will increase, but *medium confidence* in the magnitude of mean change.

Table 4.6: Projected changes in the annual and seasonal mean climate for the eastern Federated States of Micronesia under four emissions scenarios; RCP2.6 (very low emissions, in dark blue), RCP4.5 (low emissions, in light blue), RCP6 (medium emissions, in orange) and RCP8.5 (very high emissions, in red). Projected changes are given for four 20-year periods centred on 2030, 2050, 2070 and 2090, relative to a 20-year period centred on 1995. Values represent the multi-model mean change, with the 5–95% range of uncertainty in brackets. Confidence in the magnitude of change is expressed as *high*, *medium* or *low*. Surface air temperatures in the Pacific are closely related to sea-surface temperatures (SST), so the projected changes to air temperature given in this table can be used as a guide to the expected changes to SST. (See also Section 1.5.2). 'NA' indicates where data are not available.

Variable	Season	2030	2050	2070	2090	Confidence (magnitude of change)
Surface air temperature (°C)	Annual	0.7 (0.4–0.9)	0.8 (0.6–1.2)	0.8 (0.5–1.2)	0.8 (0.5–1.2)	*High*
		0.7 (0.5–1)	1.1 (0.8–1.4)	1.4 (1–1.9)	1.5 (1–2.1)	
		0.6 (0.4–0.9)	1 (0.7–1.4)	1.4 (1–2)	1.8 (1.3–2.6)	
		0.8 (0.6–1.1)	1.4 (1–1.9)	2.2 (1.6–3.1)	3 (2.1–4.1)	
Maximum temperature (°C)	1-in-20 year event	0.6 (0.1–1.1)	0.7 (0.3–1.2)	0.7 (0.3–1.1)	0.8 (0.3–1.1)	*Medium*
		0.6 (0.2–0.9)	0.9 (0.5–1.4)	1.2 (0.7–1.6)	1.3 (0.9–2.1)	
		NA (NA–NA)	NA (NA–NA)	NA (NA–NA)	NA (NA–NA)	
		0.8 (0.3–1.1)	1.4 (0.8–2.2)	2.3 (1.4–3.4)	3.1 (2–4.3)	
Minimum temperature (°C)	1-in-20 year event	0.6 (0.4–0.9)	0.8 (0.5–1.3)	0.8 (0.4–1)	0.8 (0.3–1.1)	*Medium*
		0.7 (0.4–0.9)	1 (0.7–1.3)	1.3 (0.9–1.8)	1.4 (1–1.8)	
		NA (NA–NA)	NA (NA–NA)	NA (NA–NA)	NA (NA–NA)	
		0.8 (0.5–1.1)	1.5 (1–2.1)	2.3 (1.7–3.2)	3.2 (2.3–4.3)	
Total rainfall (%)	Annual	3 (-3–9)	4 (-5–13)	6 (2–14)	6 (0–11)	*Medium*
		3 (-5–12)	5 (-1–12)	7 (1–20)	6 (-2–13)	
		3 (-3–9)	4 (-2–9)	5 (-5–12)	7 (-3–17)	
		3 (1–9)	6 (1–14)	8 (3–18)	12 (3–23)	
Total rainfall (%)	Nov-Apr	2 (-7–10)	3 (-7–10)	4 (-3–16)	6 (-2–15)	*Medium*
		1 (-12–15)	3 (-4–13)	5 (-5–16)	2 (-8–12)	
		2 (-6–10)	2 (-7–7)	4 (-8–18)	5 (-10–16)	
		1 (-5–6)	3 (-7–15)	4 (-8–13)	7 (-10–21)	
Total rainfall (%)	May-Oct	4 (-1–10)	5 (-3–15)	7 (1–13)	7 (1–14)	*Medium*
		4 (-3–10)	7 (1–14)	9 (-1–18)	9 (2–17)	
		3 (-3–12)	6 (-2–16)	7 (-1–13)	10 (-2–21)	
		5 (-1–12)	9 (2–16)	12 (-1–23)	18 (2–29)	
Aragonite saturation state (Ωar)	Annual	-0.3 (-0.6–0.0)	-0.4 (-0.7–-0.1)	-0.4 (-0.6–-0.1)	-0.3 (-0.6–-0.1	*Medium*
		-0.3 (-0.6–-0.1)	-0.5 (-0.8–-0.3)	-0.7 (-0.9–-0.5)	-0.8 (-1.0–-0.5)	
		NA (NA–NA)	NA (NA–NA)	NA (NA–NA)	NA (NA–NA)	
		-0.4 (-0.6–-0.1)	-0.7 (-1.0–-0.5)	-1.1 (-1.4–-0.9)	-1.5 (-1.7–-1.3)	
Mean sea level (cm)	Annual	13 (8–18)	22 (14–30)	32 (20–45)	42 (24–60)	*Medium*
		12 (8–17)	22 (14–31)	35 (22–49)	48 (30–68)	
		12 (7–17)	22 (14–30)	34 (22–48)	49 (31–69)	
		13 (8–18)	26 (17–35)	43 (28–59)	64 (41–90)	

Table 4.7: Projected changes in the annual and seasonal mean climate for the western Federated States of Micronesia under four emissions scenarios; RCP2.6 (very low emissions, in dark blue), RCP4.5 (low emissions, in light blue), RCP6 (medium emissions, in orange) and RCP8.5 (very high emissions, in red). Projected changes are given for four 20-year periods centred on 2030, 2050, 2070 and 2090, relative to a 20-year period centred on 1995. Values represent the multi-model mean change, with the 5–95% range of uncertainty in brackets. Confidence in the magnitude of change is expressed as *high*, *medium* or *low*. Surface air temperatures in the Pacific are closely related to sea-surface temperatures (SST), so the projected changes to air temperature given in this table can be used as a guide to the expected changes to SST. (See also Section 1.5.2). 'NA' indicates where data are not available.

Variable	Season	2030	2050	2070	2090	Confidence (magnitude of change)
Surface air temperature (°C)	Annual	0.7 (0.5–0.9)	0.8 (0.6–1.1)	0.8 (0.5–1.2)	0.8 (0.4–1.2)	*High*
		0.7 (0.5–1)	1 (0.8–1.4)	1.3 (1–1.8)	1.5 (1–2.1)	
		0.6 (0.4–0.9)	1 (0.7–1.4)	1.4 (1.1–1.9)	1.8 (1.4–2.6)	
		0.8 (0.6–1.1)	1.4 (1.1–1.9)	2.2 (1.6–3.1)	3 (2.1–4)	
Maximum temperature (°C)	1-in-20 year event	0.6 (0.4–1)	0.8 (0.4–1.1)	0.7 (0.3–1.1)	0.8 (0.2–1.1)	*Medium*
		0.7 (0.3–0.9)	1 (0.5–1.3)	1.3 (0.8–1.6)	1.3 (0.8–2)	
		NA (NA–NA)	NA (NA–NA)	NA (NA–NA)	NA (NA–NA)	
		0.8 (0.4–1.1)	1.5 (0.9–2.1)	2.3 (1.5–3.2)	3.2 (2–4.3)	
Minimum temperature (°C)	1-in-20 year event	0.7 (0.4–0.8)	0.8 (0.5–1.1)	0.8 (0.4–1)	0.8 (0.4–1)	*Medium*
		0.7 (0.3–0.8)	1 (0.7–1.2)	1.2 (0.8–1.7)	1.4 (1–1.7)	
		NA (NA–NA)	NA (NA–NA)	NA (NA–NA)	NA (NA–NA)	
		0.8 (0.5–1.1)	1.5 (1–2)	2.3 (1.7–3.2)	3.2 (2.2–4.1)	
Total rainfall (%)	Annual	3 (-3–8)	3 (-4–8)	3 (-1–8)	3 (-1–8)	*Medium*
		3 (-4–8)	4 (-3–12)	6 (-3–13)	4 (-4–10)	
		0 (-6–5)	3 (-1–8)	3 (-6–10)	5 (-4–15)	
		2 (-1–7)	5 (-1–15)	7 (0–12)	10 (0–27)	
Total rainfall (%)	Nov-Apr	3 (-4–10)	2 (-6–12)	2 (-6–9)	2 (-5–11)	*Medium*
		2 (-7–11)	3 (-9–12)	5 (-7–27)	3 (-8–13)	
		1 (-5–7)	2 (-4–6)	3 (-10–12)	4 (-11–17)	
		2 (-4–8)	4 (-6–20)	4 (-11–15)	7 (-10–28)	
Total rainfall (%)	May-Oct	3 (-2–7)	5 (-1–14)	5 (-3–13)	4 (0–10)	*Medium*
		3 (0–9)	5 (-2–13)	7 (-1–14)	6 (-1–13)	
		1 (-5–5)	5 (-2–17)	4 (-3–12)	7 (-3–17)	
		3 (0–6)	7 (-2–18)	10 (-3–22)	14 (-2–31)	
Aragonite saturation state (Ωar)	Annual	-0.3 (-0.6–0.0)	-0.4 (-0.7–-0.1)	-0.4 (-0.7–-0.1)	-0.3 (-0.6–-0.1)	*Medium*
		-0.3 (-0.6–0.0)	-0.5 (-0.8–-0.3)	-0.7 (-0.9–-0.4)	-0.7 (-1.0–-0.5)	
		NA (NA–NA)	NA (NA–NA)	NA (NA–NA)	NA (NA–NA)	
		-0.4 (-0.6–-0.1)	-0.7 (-1.0–-0.4)	-1.1 (-1.3–-0.8)	-1.4 (-1.7–-1.2)	
Mean sea level (cm)	Annual	13 (8–18)	22 (14–30)	32 (20–45)	42 (24–60)	*Medium*
		12 (8–17)	22 (14–31)	35 (22–49)	48 (30–68)	
		12 (7–17)	22 (14–30)	34 (22–48)	49 (31–69)	
		13 (8–18)	26 (17–35)	43 (28–59)	64 (41–90)	

Waves Projections Summary

Table 4.8: Projected average changes in wave height, period and direction in the eastern Federated States of Micronesia for December–March and June–September for RCP4.5 (low emissions, in blue) and RCP8.5 (very high emissions, in red), for two 20-year periods (2026–2045 and 2081–2100), relative to a 1986–2005 historical period. The values in brackets represent the 5th to 95th percentile range of uncertainty.

Variable	Season	2035	2090	Confidence (range)
Wave height change (m)	December–March	-0.0 (-0.2–0.2) -0.1 (-0.3–0.2)	-0.1 (-0.3–0.1) -0.2 (-0.4–-0.0)	*Low*
	June–September	+0.0 (-0.2–0.2) +0.0 (-0.1–0.2)	0.0 (-0.2–0.2) +0.0 (-0.1–0.2)	*Low*
Wave height change (ft)	December–March	-0.1 (-0.8–0.7) -0.2 (-1.0–0.7)	-0.3 (-1.0–0.4) -0.7 (-1.2–-0.1)	*Low*
	June–September	+0.0 (-0.7–0.7) +0.0 (-0.4 to 0.6)	0.0 (-0.6 to 0.6) +0.0 (-0.5 to 0.8)	*Low*
Wave period change (s)	December–March	-0.1 (-0.6–0.4) -0.1 (-0.6–0.5)	-0.1 (-0.7–0.5) -0.2 (-0.9–0.4)	*Low*
	June–September	0.0 (-0.6–0.6) -0.0 (-0.6–0.5)	-0.0 (-0.7–0.6) -0.1 (-0.7–0.5)	*Low*
Wave direction change (° clockwise)	December–March	0 (-10–10) 0 (-10–10)	0 (-10–10) 0 (-10–10)	*Low*
	June–September	+0 (-20–40) 0 (-20–40)	+0 (-20–30) +10 (-20–60)	*Low*

Table 4.9: Projected average changes in wave height, period and direction in the western Federated States of Micronesia for December–March and June–September for RCP4.5 (low emissions, in blue) and RCP8.5 (very high emissions, in red), for two 20-year periods (2026–2045 and 2081–2100), relative to a 1986–2005 historical period. The values in brackets represent the 5th to 95th percentile range of uncertainty.

Variable	Season	2035	2090	Confidence (range)
Wave height change (m)	December–March	-0.0 (-0.3–0.2) -0.0 (-0.3–0.2)	-0.1 (-0.3–0.1) -0.2 (-0.4–0.0)	*Low*
	June–September	0.0 (-0.2–0.2) 0.0 (-0.2 to0.2)	0.0 (-0.2–0.2) 0.0 (-0.2–0.2)	*Low*
Wave height change (ft)	December–March	-0.1 (-0.8–0.7) -0.1 (-0.9–0.7)	-0.3 (-1.0–0.5) -0.7 (-1.3–0.0)	*Low*
	June–September	0.0 (-0.6–0.6) 0.0 (-0.4–0.7)	0.0 (-0.4–0.7) 0.0 (-0.3–0.8)	*Low*
Wave period change (s)	December–March	-0.1 (-0.4–0.3) -0.1 (-0.5–0.3)	-0.1 (-0.5–0.3) -0.3 (-0.7–0.2)	*Low*
	June–September	0.0 (-0.4–0.4) 0.0 (-0.4–0.4)	-0.0 (-0.5–0.4) -0.1 (-0.6–0.4)	*Low*
Wave direction change (° clockwise)	December–March	0 (-5–5) 0 (-5–5)	0 (-10–5) -0 (-10–5)	*Low*
	June–September	+0 (-40–40) 0 (-40–40)	+0 (-30–40) +10 (-30–50)	*Low*

Wind-wave variables parameters are calculated for a 20-year period centred on 2035.